ORIGINAL RESEARCH

Relationship Between Endothelial Wall Shear Stress and High-Risk Atherosclerotic Plaque Characteristics for Identification of Coronary Lesions That Cause Ischemia: A Direct Comparison With Fractional Flow Reserve

Donghee Han, MD; Anna Starikov, MD; Bríain ó Hartaigh, PhD; Heidi Gransar, MS; Kranthi K. Kolli, PhD; Ji Hyun Lee, MD; Asim Rizvi, MD; Lohendran Baskaran, MD; Joshua Schulman-Marcus, MD; Fay Y. Lin, MD; James K. Min, MD, FACC

***Background*—**Wall shear stress (WSS) is an established predictor of coronary atherosclerosis progression. Prior studies have reported that high WSS has been associated with high-risk atherosclerotic plaque characteristics (APCs). WSS and APCs are quantifiable by coronary computed tomography angiography, but the relationship of coronary lesion ischemia—evaluated by fractional flow reserve—to WSS and APCs has not been examined.

***Methods and Results*—**WSS measures were obtained from 100 evaluable patients who underwent coronary computed tomography angiography and invasive coronary angiography with fractional flow reserve. Patients were categorized according to tertiles of mean WSS values defined as low, intermediate, and high. Coronary ischemia was defined as fractional flow reserve ≤0.80. Stenosis severity was determined by minimal luminal diameter. APCs were defined as positive remodeling, low attenuation plaque, and spotty calcification. The likelihood of having positive remodeling and low-attenuation plaque was greater in the high WSS group compared with the low WSS group after adjusting for minimal luminal diameter (odds ratio for positive remodeling: 2.54, 95% CI 1.12–5.77; odds ratio for low-attenuation plaque: 2.68, 95% CI 1.02–7.06; both $P<0.05$). No significant relationship was observed between WSS and fractional flow reserve when adjusting for either minimal luminal diameter or APCs. WSS displayed no incremental benefit above stenosis severity and APCs for detecting lesions that caused ischemia (area under the curve for stenosis and APCs: 0.87, 95% CI 0.81–0.93; area under the curve for stenosis, APCs, and WSS: 0.88, 95% CI 0.82–0.93; $P=0.30$ for difference).

***Conclusions*—**High WSS is associated with APCs independent of stenosis severity. WSS provided no added value beyond stenosis severity and APCs for detecting lesions with significant ischemia. **(*J Am Heart Assoc*. 2016;5:e004186 doi: 10.1161/JAHA.116.004186)**

Key Words: coronary computed tomography angiography • fractional flow reserve • plaque vulnerability • wall shear stress

Atherosclerosis is a major cause of cardiovascular disease and is the foremost cause of morbidity and mortality worldwide.[1,2] Endothelial wall shear stress (WSS) reflects a parallel hemodynamic force that resides within the endothelial surface of the arterial wall.[3] By a complex array of cellular, molecular, and biochemical reactions, WSS affects the structure of blood vessels.[4–6] Prior studies have documented that high WSS is a key component in atherosclerotic plaque destabilization, arterial wall remodeling, and atherosclerosis progression.[7–9]

Coronary computed tomography angiography (CCTA) is a noninvasive imaging method that enables determination of anatomic atherosclerotic plaque characteristics (APCs), including coronary stenosis severity, arterial positive remodeling (PR), low-attenuation plaque (LAP), and spotty calcification (SC).[10–12] Recent developments in computational fluid dynamics (CFD) applied to CCTA enable determination of physiological coronary processes, including WSS.[13]

Fractional flow reserve (FFR) represents the current gold standard for determining coronary lesion–specific ischemia,

From the Department of Radiology, Dalio Institute of Cardiovascular Imaging, NewYork-Presbyterian Hospital and the Weill Cornell Medicine, New York, NY (D.H., A.S., B.H., K.K.K., J.H.L., A.R., L.B., J.S.-M., F.Y.L., J.K.M.); Department of Imaging, Cedars Sinai Medical Center, Los Angeles, CA (H.G.).

Correspondence to: James K. Min, MD, FACC, Dalio Institute of Cardiovascular Imaging, New York-Presbyterian Hospital and the Weill Cornell Medicine, 413 E. 69th Street, Suite 108, New York, NY 10021. E-mail: jkm2001@med.cornell.edu

Received July 20, 2016; accepted November 3, 2016.

and its use to guide decision making for coronary revascularization results in improved event-free survival.[14] Prior reports have elicited stenosis severity and APCs by CCTA to be important and independent factors for identification of ischemia-causing lesions compared with FFR.[15,16] To date, the association of WSS to CCTA APCs and coronary ischemia has not been evaluated. Consequently, we sought to evaluate the independent relationship between WSS and coronary ischemia as determined by FFR, the reference standard.

Methods

Study Population

The DeFACTO (Determination of Fractional Flow Reserve by Anatomic Computed Tomographic Angiography; NCT01233518) study is a prospective multicenter trial performed at 17 centers in 5 countries (Canada, n=1; Belgium, n=1; Latvia, n=1; South Korea, n=2; and United States, n=12).[17] For the purpose of this investigation, 100 patients with suspected coronary artery disease enrolled in the DeFACTO trial were selected from a post hoc sample size calculation and subsequently evaluated. Invasive coronary angiography (ICA) with intended FFR was performed within 60 days of CCTA, and no intervening coronary events were observed. Patients were not deemed eligible for participation if they had a prior history of coronary artery bypass grafting, percutaneous coronary intervention with suspected in-stent restenosis based on CCTA findings, contraindication to adenosine, suspicion of or recent acute coronary syndrome, complex congenital heart disease, pacemaker or defibrillator, prosthetic heart valve, significant arrhythmia, serum creatinine level >1.5 mg/dL, allergy to iodinated contrast, pregnant state, body mass index >35, evidence of active clinical instability or life-threatening disease, or an inability to adhere to study procedures. The appropriate institutional review board committees approved the study protocol, and all patients provided written informed consent.

ICA and FFR Measurement

Selective ICA was performed by standard protocol in accordance with the American College of Cardiology guidelines for coronary angiography, with a minimum of 2 projections obtained per vessel distribution and with angles of projection optimized according to the cardiac position. FFR was assessed at the time of ICA in vessels deemed clinically indicated for evaluation and demonstrating an ICA stenosis between 30% and 90%. After administration of intracoronary nitroglycerin, a pressure-monitoring guide wire (PressureWire Certus [St. Jude Medical Systems] or ComboWire [Volcano Corp]) was inserted distal to a stenosis. Hyperemia was induced with intravenous administration of adenosine at a rate of 140 μg/kg per minute. FFR was calculated by dividing the mean distal coronary pressure by the mean aortic pressure during hyperemia. In accordance with prior multicenter studies, FFR at a threshold of ≤0.80 was considered significant to indicate lesion-specific ischemia.

CCTA Scan and Plaque Analysis

CCTA was performed with single- or dual-source computed tomography scanners using ≥64 detector rows with prospective or retrospective electrocardiographic gating in direct accordance with the Society of Cardiovascular Computed Tomography guidelines on performance of CCTA.[18,19] An intravenous contrast agent (≈80–100 mL) followed by saline (50–80 mL) was injected at a flow rate of 5 mL/s. The scan parameters included heart rate–dependent pitch (0.20–0.45), 330-ms gantry rotation time, 100 or 120 kVp tube voltage, and 350 to 800 mA tube current. Transaxial images were reconstructed with 0.5- to 0.75-mm slice thickness, 0.3-mm slice increment, 160- to 250-mm field of view, 512×512 matrix, and a standard kernel. A more in-depth description of the plaque analysis methods was provided previously.[16] In brief, CCTA images were analyzed using QAngio CT Research Edition (v2.1.9.1; Medis Medical Imaging Systems BV) in a semiautomated manner. Quantitative measurements include lesion length and degree of coronary stenosis (ie, minimal luminal area, minimal luminal diameter, area stenosis, and diameter stenosis). Diameter stenosis (as percentage) and area stenosis (as percentage) were calculated using proximal and distal reference segments. Minimal lumen diameter (MLD; in mm) and minimal lumen area (in mm^2) were measured respectively from the long-axis and short-axis views of double-oblique reconstructions at the site of the maximal stenosis. Percentage of aggregate plaque volume was defined as the aggregate plaque volume divided by the total vessel volume.[15] Plaque characteristics were qualitatively assessed according to PR, LAP, and SC. A remodeling index was defined as a maximal lesion vessel diameter divided by the proximal reference vessel diameter. PR was defined as a remodeling index >1.1. LAP was defined as any voxel <30 Hounsfield units within a coronary plaque. An intralesion calcific plaque <3 mm in length that composed <90° of the lesion circumference defined SC.

Calculation of Endothelial WSS From CCTA

Patient-specific 3-dimensional geometry of the coronary artery was reconstructed from CCTA imaging data. Following the 3-dimensional reconstruction, blood flow simulations were performed by solving Navier-Stokes equations. WSS by CFD analysis involved 3 primary steps: (1) volumetric coronary tree

mesh generation, (2) specification of physiological boundary conditions for blood flow simulations, and (3) numerical computation of WSS by solving of the Navier-Stokes equations. Hyperemic resistances were prescribed by reducing the microcirculatory resistances in accordance with the effects of adenosine.[20] WSS was calculated from the velocity solution at each mesh point on the lateral wall and was postprocessed and rendered with a blue-to-red color map for visual analysis in ParaView (www.paraview.org) (Figure 1).

Coregistration Between CCTA and the 3-Dimensional Reconstructed WSS Model

In total, 100 patients (n=163 coronary lesions) with evaluable CCTAs were indiscriminately selected for calculation of WSS. Stenotic lesions were determined by semiquantitative assessment using 3-dimensional reconstructed coronary geometries, and corresponding lesions were identified in ICA images with invasive FFR evaluation. For each lesion, a sphere with a radius of 0.5 cm was placed at the center of the maximal stenosis as a region of interest. The magnitude of the WSS within each region of interest was calculated. The mean of the calculated magnitude was used to define the average level of WSS for a particular lesion. For the purpose of this study, the mean of WSS was categorized according to tertiles.

Statistical Methods

Continuous variables are expressed as mean±SD, and categorical variables are reported as counts with proportions. Comparisons between WSS groups were assessed by use of a 1-way ANOVA for continuous variables in which subsequent multiple pairwise comparisons were adjusted using the Sidak method and Pearson's chi-square test for categorical variables. The Student unpaired *t* test was performed for comparison of covariates between 2 groups. Correlation analysis was performed using Pearson's correlation coefficient, whereas adjusted linear regression reporting β coefficients and standard errors was also performed to report the linear relationship between WSS and ICA stenosis. Logistic regression analyses reporting odds ratios with 95% CIs were performed to predict the likelihood of having APCs according to the WSS groups. Candidate variables related to coronary stenosis (ie, minimal lumen area, MLD, area stenosis, diameter stenosis) and each APC (ie, PR, LAP, and SC) were tested for entry to the multivariate model, with $P<0.1$ for association with WSS; next, backward-stepwise regression was performed to construct a multivariate model with a threshold of $P<0.05$.[21,22] After an elimination approach, MLD was selected in variables related to coronary stenosis, and PR and LAP were selected in variables related to APCs. WSS was combined with stenosis severity in model 1, with APCs in model 2, and with both stenosis severity and APCs in model 3. The receiver operating characteristic curve was fashioned to evaluate the discriminatory ability of WSS for predicting ischemia, and areas under the receiver operating characteristic curve were compared using the method described by DeLong et al.[23] The latter method is a nonparametric test for comparing correlated areas under the receiver operating characteristic curve by using the generalized *U* statistics to generate an estimated covariance matrix. For the primary hypothesis of an association between WSS and FFR, sample size calculation was performed using a 2-sided sample equal variance test with WSS as a categorical variable. We estimated that 34 lesions were required to achieve a statistical power of 80% with an α level of 0.05. For the

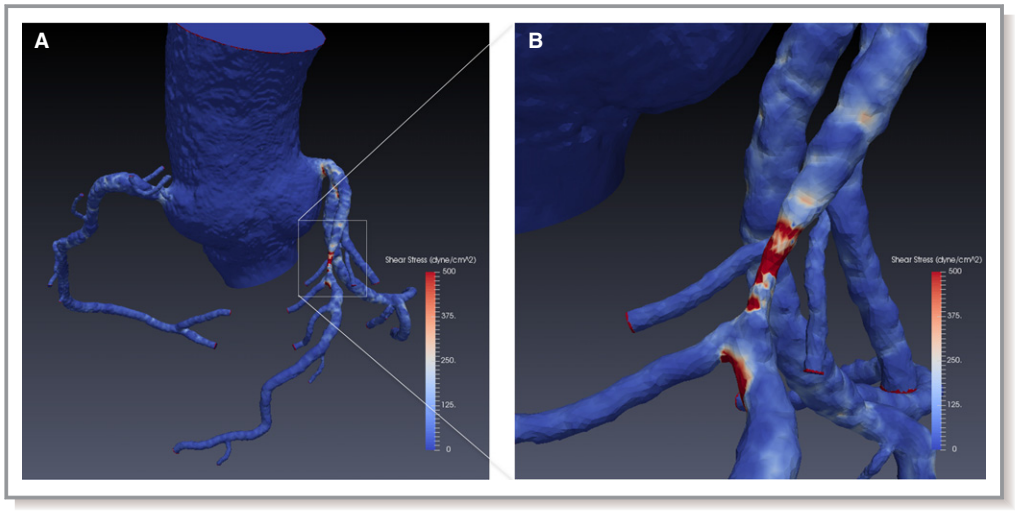

Figure 1. A, Color-encoded wall shear stress based on a 3-dimensional model by coronary computed tomography angiography. B, Zoomed image for coronary atherosclerotic lesion.

secondary hypothesis of an association between WSS and APCs, we estimated that 41 lesions for PR, 34 lesions for LAP, and 42 lesions for SC were required to detect a statistical power of 80% with an α level of 0.05, based on the equality of 2 independent proportions test. A 2-tailed $P<0.05$ was considered statistically significant. All statistical analyses were performed using STATA version 13 (StataCorp LP).

Results

The mean age of the current study population was 62.8±9.1 years, and the study sample was predominantly male (70%) (Table 1). Tertiles of mean WSS were partitioned at low (range 5–146 dyne/cm^2), intermediate (range 146–259 dyne/cm^2), and high (range 259–891 dyne/cm^2) (Table 2). Mean WSS values according to low, intermediate, and high WSS groups were 89.2±36.1, 188.9±31.0, and 408.7±132.7 dyne/cm^2, respectively. Most clinical characteristics did not differ significantly between WSS groups. For lesion characteristics, diameter stenosis, area stenosis, MLD, and minimal lumen area were associated with WSS groups; lesion location, length, and plaque volume were not associated with WSS (Table 2).

Relationship Between Stenosis Severity by ICA and CCTA WSS

ICA stenosis in the high WSS group (55±13.4%) was significantly greater compared with the low (43.4±18.3%) and intermediate WSS groups (47.6±12.2%) (Figure 2A). The correlation coefficient between WSS and ICA stenosis displayed significant correlation ($r=0.341$, $P<0.001$) (Figure 2B). Multivariable linear regression revealed that WSS was an independent predictor of increasing ICA stenosis (eg, $\beta=1.7$, SE 0.08 [per 10 dyne/cm^2], $P=0.028$), even after adjusting for APCs.

Table 1. Baseline Characteristics of Study Population

Age, y	62.8±9.1
Male	70 (70%)
BSA	1.9±0.3
Race	
White	67 (67%)
Other	33 (33%)
Diabetes mellitus	18 (18%)
Hypertension	73 (73%)
Hyperlipidemia	80 (80%)
Family history of CAD	16 (16%)
Current smoker	23 (23%)

BSA indicates body surface area; CAD, coronary artery disease.

Relationship Between CCTA APCs and CCTA WSS

PR, LAP, and SC by CCTA were observed in 71 (43.6%), 37 (22.7%), and 21 (12.9%) of 163 lesions, respectively. Prevalence of PR and LAP increased with higher WSS ($P=0.006$ and $P=0.002$, respectively), whereas SC did not ($P=0.309$) (Figure 3A). Increasing numbers of intraplaque APCs were associated with high WSS ($P=0.006$) (Figure 3B). The odds of PR or LAP presence, as well as the presence of any APC

Table 2. Clinical and Lesion Characteristics According to WSS Groups

	Low (n=55)	Intermediate (n=54)	High (n=54)	*P* Value
Age, y	62.1±7.6	61.7±10.2	62.9±8.9	0.758
Male	36 (65.5)	43 (79.6)	40 (74.1)	0.244
BSA	1.9±0.3	1.9±0.2	1.9±0.2	0.457
Race (white)	40 (72.7)	40 (74.1)	36 (66.7)	0.784
Hypertension	40 (72.7)	36 (66.7)	40 (74.1)	0.773
Diabetes mellitus	13 (23.6)	7 (13.0)	9 (16.7)	0.334
Lesion characteristics				
Location				0.102
Proximal	31 (56.4)	21 (38.9)	30 (55.6)	
Mid	16 (29.1)	22 (40.7)	21 (38.9)	
Distal	8 (14.6)	11 (20.4)	3 (5.6)	
Epicardial				0.322
LAD	28 (50.9)	32 (59.3)	27 (50.0)	
LCX	16 (29.1)	13 (24.1)	10 (18.5)	
RCA	11 (20.0)	9 (16.7)	17 (31.5)	
Lesion length	23.2±12.9	24.9±12.1	24.3±10.4	0.740
Minimal lumen area	3.7±2.1	2.7±1.4	2.5±1.4	<0.001
Minimal lumen diameter	2.1±0.6	1.8±0.5	1.7±0.5	<0.001
Area stenosis	56.1±1 8.3	59.3±16.5	67.1±17.6	0.004
Diameter stenosis	35.3±14.7	37.5±12.7	44.4±14.3	0.002
%APV	54.9±16.3	54.4±8.6	57.9±19.4	0.435
Mean WSS	89.2±36.1	188.9±31.0	408.7±132.7	<0.001
WSS range	5.0–146.1	146.6–259.3	259.5–890.9	

APV indicates aggregate plaque volume; BSA, body surface area; LAD, left anterior descending; LCX, left circumflex; RCA, right coronary artery; WSS, wall shear stress.

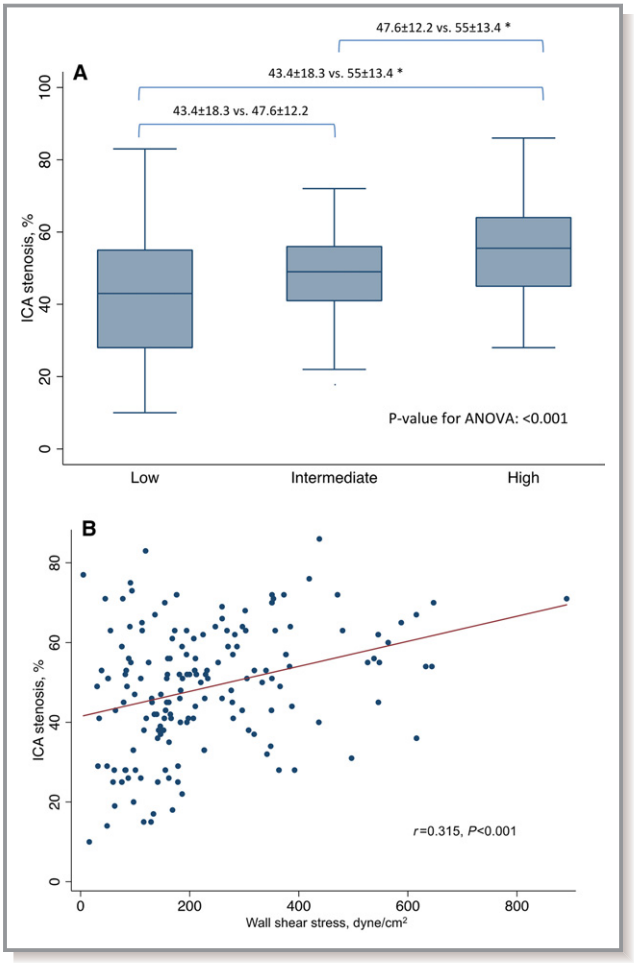

Figure 2. A, Box plots reporting mean maximal ICA stenosis values according to WSS groups. B, Linear regression analysis of the correlation between WSS and ICA stenosis. *P<0.05. ANOVA indicates 1-way analysis of variance for continuous variables; ICA, invasive coronary angiography; WSS, wall shear stress.

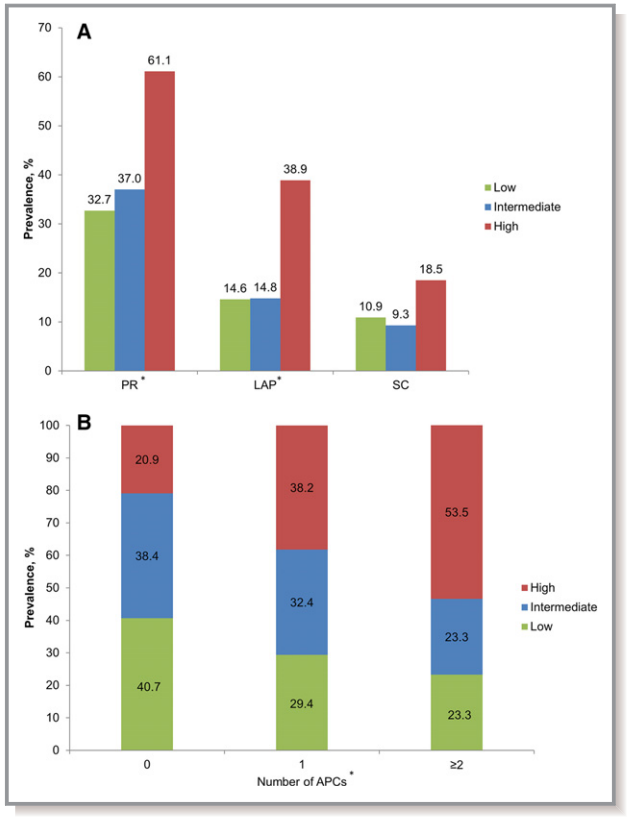

Figure 3. A, Prevalence of PR, LAP, and SC according to WSS groups. B, Number of APCs according to WSS groups. *P<0.05. APCs indicates atherosclerotic plaque characteristics; LAP, low-attenuation plaque; PR, positive remodeling; SC, spotty calcification; WSS, wall shear stress.

feature, were higher in the highest WSS group compared with the lowest WSS group (Table 3). SC was not associated with WSS groups in univariable or multivariable models (Table 3). No significant differences in the likelihood of APC presence were noted for intermediate versus low WSS.

Stenosis Severity, APC, and WSS for Identification of FFR

In total, 60 (36.8%) lesions presented with significant ischemia. FFR values and WSS were inversely related. FFR in the high WSS group was significantly lower compared with the low WSS group (eg, 0.79±0.13 versus 0.86±0.13, P=0.011). In univariable analyses, MLD, minimal lumen area, diameter stenosis, area stenosis, APCs, and WSS were associated with FFR-defined ischemic lesions, but WSS was not evident in multivariable models (Table 4). As listed in Figure 4, improved discrimination of ischemia was observed when adding APCs to MLD compared with MLD alone (area under the receiver operating characteristic curve 0.87 [95% CI 0.81–0.93] for MLD, PR, and LAP versus 0.72 [95% CI 0.64–0.80] for MLD alone; P<0.001 for difference). No incremental discriminatory value of coronary ischemia was observed when adding WSS to the model comprising MLD, PR, and LAP (area under the receiver operating characteristic curve 0.88 [95% CI 0.82–0.93] for MLD, PR, LAP, and WSS; P=0.297 for difference versus MLD, PR, and LAP).

Discussion

In this present study, high WSS was independently associated with stenosis severity and APCs. In particular, high WSS portended ≈2.5-fold increased odds of PR and LAP presence, even after adjustment of coronary stenosis severity. In contrast, WSS was not an independent predictor of coronary ischemia and added no predictive value for determining ischemia beyond stenosis severity and APCs. To our knowledge, these data are the first to explore the relationship between APCs and WSS for precise identification of coronary lesions with significant ischemia by invasive FFR and to refute the notion that WSS

Table 3. Logistic Regression for the Likelihood of Having APCs According to WSS Groups

	Unadjusted			Adjusted by Stenosis*		
	OR	95% CI	*P* Value	OR	95% CI	*P* Value
Positive remodeling						
Low group	1	Reference		1	Reference	
Intermediate group	1.21	0.55–2.66	0.637	0.99	0.43–2.24	0.973
High group	3.23	1.47–7.08	0.003	2.54	1.12–5.77	0.026
Low attenuated plaque						
Low group	1	Reference		1	Reference	
Intermediate group	1.02	0.35–2.95	0.968	0.76	0.25–2.28	0.623
High group	3.74	0.48–9.46	0.005	2.68	1.02–7.06	0.046
Spotty calcification						
Low group	1	Reference		1	Reference	
Intermediate group	0.83	0.24–2.9	0.775	0.71	0.20–2.56	0.601
High group	1.86	0.62–5.53	0.267	1.52	0.48–4.76	0.473
Presence of any APCs						
Low group	1	Reference		1	Reference	
Intermediate group	1.11	0.51–2.42	0.786	0.89	0.40–2.01	0.782
High group	3.5	1.59–7.70	0.002	2.72	1.19–6.19	0.017

Adjusted by minimal lumen diameter. APCs indicates adverse plaque characteristics; OR, odds ratio; WSS, wall shear stress.

can be used as a diagnostic parameter for improved discrimination of ischemia-causing coronary lesions by CCTA.

Previous studies have reported that high WSS is closely related to high-risk APCs. Samady and colleagues reported that high WSS assessed by intravascular ultrasound images is associated with longitudinal development of high-risk APCs, including intraplaque necrotic core or expansive arterial remodeling.[8] Indeed, the incidence of expansive remodeling in high WSS coronary segments is 2-fold higher compared with low WSS segments. Noninvasive imaging has been similarly examined for these findings. Hetterich and coworkers reported the feasibility of applying CFD techniques to CCTA for determining WSS.[24] In their study, higher WSS was associated with APCs and vessel wall thickness. Our present study findings directly expand on these data by demonstrating that high WSS is related to the presence of APCs and is inversely proportional to FFR values. This direct relationship, however, is not an independent factor deserving of consideration for identification of coronary artery lesions that cause ischemia.

In this present study, it is unsurprising that WSS is directly related to coronary lesion stenosis severity because WSS is a direct product of hemodynamic blood flow.[25] For APCs, this information was heretofore unclear. We assessed 3 APCs that were previously identified as being directly related to ischemia and incremental to stenosis severity for enhanced diagnosis compared with an invasive FFR reference standard (eg, PR, LAP, and SC).[16] Although beyond the scope of this study, there is an array of possible cellular explanations for these study findings. Germane to PR, high WSS stimulates endothelial macrophages, which in turn produce metalloproteinases.[26] These metalloproteinases further increase the extraluminal area and remodeling index in lesions with high WSS.[27,28] High WSS also suppresses vascular smooth muscle cell proliferation and induces apoptosis by augmenting transforming growth factor β and nitric oxide within endothelial cells.[29,30] These processes potentially contribute to transformation of APCs to a more high-risk state in which LAP, a CCTA surrogate of intraplaque necrotic core, may be more likely present. Early studies have suggested SC as another high-risk plaque associated with coronary ischemia, although more recent studies have negated this view.[31–33] The relationship between SC and other important coronary artery disease findings, including ischemia and future acute coronary syndromes, does not yet appear to be fully defined. In the current study, PR and LAP were found to be associated with high WSS, whereas SC did not display any notable relationship in lesions with either low or high WSS. Yet, high WSS promotes vascular calcification by increasing the expression of bone morphogenic protein 4, and it seems reasonable to consider SC an imaging surrogate of such a process.[34] It is possible—and may be likely, based on the current study results—that this is a parallel process that occurs in association with the development and presence of PR and LAP but is less influential in the development of ischemia.

Table 4. Logistic Regression for Detection of Lesions With Significant Ischemia

	OR	95% CI	*P* Value
Univariable			
MLD, per 1 mm	6.99	2.99–16.35	<0.001
Diameter stenosis, per 5%	1.40	1.22–1.62	<0.001
MLA, per 1 mm^2	1.96	1.43–2.68	<0.001
Area stenosis, per 5%	1.33	1.18–1.50	<0.001
PR	13.91	6.35–30.5	<0.001
LAP	7.61	3.33–17.40	<0.001
SC	3.28	1.27–8.47	0.014
High WSS group, vs low WSS group	3.33	1.45–7.66	0.005
Multivariable			
Model 1			
MLD, per 1 mm	6.09	2.55–14.50	<0.001
High WSS group, vs low WSS group	2.08	0.85–5.12	0.110
Model 2			
PR	10.51	4.38–25.21	<0.001
LAP	3.09	1.15–8.35	0.026
High WSS group, vs low WSS group	1.79	0.64–4.96	0.265
Model 3			
MLD, per 1 mm	6.18	2.24–17.09	<0.001
PR	12.02	4.67–30.99	<0.001
LAP	2.41	0.84–6.95	0.104
High WSS group, vs low WSS group	1.34	0.45–3.99	0.436

LAP indicates low attenuation plaque; MLA, minimal luminal area; MLD, minimal luminal diameter; OR, odds ratio; PR, positive remodeling; SC, spotty calcification; WSS, wall shear stress.

Prior studies have examined the relationship of APCs to coronary ischemia independent of stenosis severity.[16] These APCs add to CFD-based calculations of FFR from CCTA. Although the precise mechanisms of how APCs may adversely affect hemodynamics have not been fully explored, it is possible that they represent imaging surrogate markers of local coronary cellular and biochemical responses at the endothelial layer.[35,36] In aggregate, these data combined with the present study findings suggest that CFD-based assessment of CCTA for coronary ischemia should be limited to FFR from CCTA and APCs, with little attention needing to be paid to WSS for measures of ischemia. In hindsight, these findings are perhaps intuitive, given that the driving forces of translesional hyperemic flow—as measured by FFR from CCTA—are orders of magnitude higher than WSS and are more likely to explain the ischemia process. Despite the

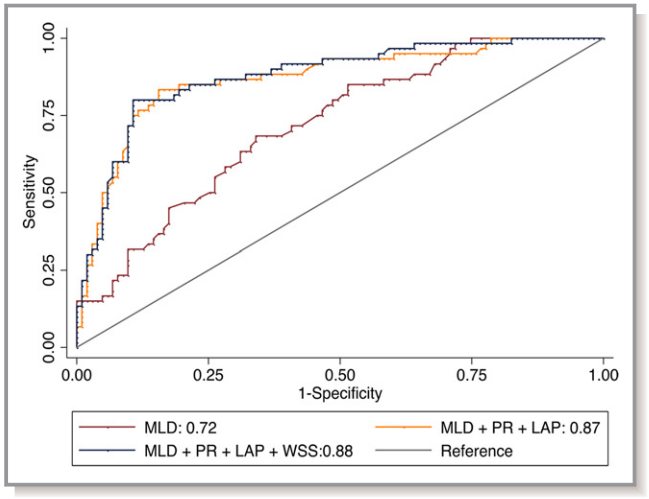

Figure 4. Receiver operating characteristic curves for stenosis severity, adverse plaque characteristics, and WSS, for predicting significant ischemia. LAP indicates low-attenuation plaque; MLD, minimal luminal diameter; PR, positive remodeling; WSS, wall shear stress.

"negative" findings that WSS do not incrementally contribute to the definition of coronary ischemia, these study findings are nevertheless essential to our understanding of the prioritization of CCTA image analyses, given the detailed and time-consuming process of WSS calculations.

Limitations

This study is not without limitations. Although this study comprised patients derived from a prospective multicenter international study, they were nevertheless representative of an indiscriminately selected group, and as such, we cannot discount the possible occurrence of a selection bias. Nevertheless, to our knowledge, this study is the largest study population size designed to investigate WSS by CFD-based application to noninvasive CCTA. The cross-sectional nature of this study limits our inference of the potential causal relationship between WSS and plaque morphology. In the present study, APCs were available only as dichotomous categorical measures. Consequently, the quantitative assessment of APCs (eg, LAP volume and remodeling index) and their possible relationship with WSS warrants further investigation. According to sample size calculations, our study sample was sufficiently sized to assess the relationship of WSS groups with FFR, PR, and LAP. Nevertheless, it bears mentioning that the relationship with SC was somewhat underpowered because SC lesions in the current study failed to exceed the number required to test for statistical significance; therefore, caution should be taken when interpreting our findings related with SC. Prior invasive studies suggest the importance of low, in addition to high, WSS for atherosclerosis progression.[7,8] Moreover, the pathophysiological understanding of WSS and its levels as a function of

high-risk APCs and atherosclerosis progression require further investigation. The calculation of WSS was derived from CCTA images and was not validated against an invasive reference standard. Yet prior studies demonstrate feasibility and generally high accuracy for CFD applied to CCTA, and in this study, we expected similar performance.[13,37] Finally, the current study was performed using a simulation of mean time-averaged flow as opposed to a pulsatile simulation over a cardiac cycle. WSS is a dynamic phenomenon that is further affected by a host of factors that alter endothelial function, and our study was unable to account for all potential contributory factors. Consequently, the present study was unable to calculate perhaps more informative variables related to shear stress, including time-varying WSS, or oscillatory shear index. Future studies examining these metrics now appear warranted.

Conclusion

In this study, we identified high WSS to be directly related to the presence and number of APCs; however, high WSS was not independently associated with coronary lesion ischemia.

Sources of Funding

This study was funded in part by a generous gift from the Dalio Institute of Cardiovascular Imaging and the Michael Wolk Foundation. The DeFACTO study was funded by HeartFlow, Inc, Redwood City, CA.

Disclosures

Dr Min has served as a consultant or on the medical advisory boards of GE Healthcare, HeartFlow, and Arineta; and has received research support from GE Healthcare. The remaining authors have no disclosures to report.

References

1. Murray CJ, Lopez AD. Measuring the global burden of disease. *N Engl J Med*. 2013;369:448–457.
2. Mozaffarian D, Benjamin EJ, Go AS, Arnett DK, Blaha MJ, Cushman M, Das SR, de Ferranti S, Despres JP, Fullerton HJ, Howard VJ, Huffman MD, Isasi CR, Jimenez MC, Judd SE, Kissela BM, Lichtman JH, Lisabeth LD, Liu S, Mackey RH, Magid DJ, McGuire DK, Mohler ER III, Moy CS, Muntner P, Mussolino ME, Nasir K, Neumar RW, Nichol G, Palaniappan L, Pandey DK, Reeves MJ, Rodriguez CJ, Rosamond W, Sorlie PD, Stein J, Towfighi A, Turan TN, Virani SS, Woo D, Yeh RW, Turner MB. Heart Disease and Stroke Statistics-2016 update: a report from the American Heart Association. *Circulation*. 2016;133:e38–e360.
3. Davies PF. Flow-mediated endothelial mechanotransduction. *Physiol Rev*. 1995;75:519–560.
4. De Keulenaer GW, Chappell DC, Ishizaka N, Nerem RM, Alexander RW, Griendling KK. Oscillatory and steady laminar shear stress differentially affect human endothelial redox state: role of a superoxide-producing NADH oxidase. *Circ Res*. 1998;82:1094–1101.
5. Gimbrone MA Jr, Topper JN, Nagel T, Anderson KR, Garcia-Cardena G. Endothelial dysfunction, hemodynamic forces, and atherogenesis. *Ann N Y Acad Sci*. 2000;902:230–239; discussion 239-240.
6. Ando J, Yamamoto K. Effects of shear stress and stretch on endothelial function. *Antioxid Redox Signal*. 2011;15:1389–1403.
7. Stone PH, Coskun AU, Kinlay S, Clark ME, Sonka M, Wahle A, Ilegbusi OJ, Yeghiazarians Y, Popma JJ, Orav J, Kuntz RE, Feldman CL. Effect of endothelial shear stress on the progression of coronary artery disease, vascular remodeling, and in-stent restenosis in humans: in vivo 6-month follow-up study. *Circulation*. 2003;108:438–444.
8. Samady H, Eshtehardi P, McDaniel MC, Suo J, Dhawan SS, Maynard C, Timmins LH, Quyyumi AA, Giddens DP. Coronary artery wall shear stress is associated with progression and transformation of atherosclerotic plaque and arterial remodeling in patients with coronary artery disease. *Circulation*. 2011;124:779–788.
9. Vergallo R, Papafaklis MI, Yonetsu T, Bourantas CV, Andreou I, Wang Z, Fujimoto JG, McNulty I, Lee H, Biasucci LM, Crea F, Feldman CL, Michalis LK, Stone PH, Jang IK. Endothelial shear stress and coronary plaque characteristics in humans: combined frequency-domain optical coherence tomography and computational fluid dynamics study. *Circ Cardiovasc Imaging*. 2014;7:905–911.
10. Budoff MJ, Dowe D, Jollis JG, Gitter M, Sutherland J, Halamert E, Scherer M, Bellinger R, Martin A, Benton R, Delago A, Min JK. Diagnostic performance of 64-multidetector row coronary computed tomographic angiography for evaluation of coronary artery stenosis in individuals without known coronary artery disease: results from the prospective multicenter ACCURACY (assessment by coronary computed tomographic angiography of individuals undergoing invasive coronary angiography) trial. *J Am Coll Cardiol*. 2008;52:1724–1732.
11. Fischer C, Hulten E, Belur P, Smith R, Voros S, Villines TC. Coronary CT angiography versus intravascular ultrasound for estimation of coronary stenosis and atherosclerotic plaque burden: a meta-analysis. *J Cardiovasc Comput Tomogr*. 2013;7:256–266.
12. Nakazato R, Shalev A, Doh JH, Koo BK, Dey D, Berman DS, Min JK. Quantification and characterisation of coronary artery plaque volume and adverse plaque features by coronary computed tomographic angiography: a direct comparison to intravascular ultrasound. *Eur Radiol*. 2013;23:2109–2117.
13. Taylor CA, Fonte TA, Min JK. Computational fluid dynamics applied to cardiac computed tomography for noninvasive quantification of fractional flow reserve: scientific basis. *J Am Coll Cardiol*. 2013;61:2233–2241.
14. Tonino PA, De Bruyne B, Pijls NH, Siebert U, Ikeno F, van' t Veer M, Klauss V, Manoharan G, Engstrom T, Oldroyd KG, Ver Lee PN, MacCarthy PA, Fearon WF. Fractional flow reserve versus angiography for guiding percutaneous coronary intervention. *N Engl J Med*. 2009;360:213–224.
15. Nakazato R, Shalev A, Doh JH, Koo BK, Gransar H, Gomez MJ, Leipsic J, Park HB, Berman DS, Min JK. Aggregate plaque volume by coronary computed tomography angiography is superior and incremental to luminal narrowing for diagnosis of ischemic lesions of intermediate stenosis severity. *J Am Coll Cardiol*. 2013;62:460–467.
16. Park HB, Heo R, o Hartaigh B, Cho I, Gransar H, Nakazato R, Leipsic J, Mancini GB, Koo BK, Otake H, Budoff MJ, Berman DS, Erglis A, Chang HJ, Min JK. Atherosclerotic plaque characteristics by CT angiography identify coronary lesions that cause ischemia: a direct comparison to fractional flow reserve. *JACC Cardiovasc Imaging*. 2015;8:1–10.
17. Min JK, Berman DS, Budoff MJ, Jaffer FA, Leipsic J, Leon MB, Mancini GB, Mauri L, Schwartz RS, Shaw LJ. Rationale and design of the DeFACTO (determination of fractional flow reserve by anatomic computed tomographic angiography) study. *J Cardiovasc Comput Tomogr*. 2011;5:301–309.
18. Halliburton SS, Abbara S, Chen MY, Gentry R, Mahesh M, Raff GL, Shaw LJ, Hausleiter J. SCCT guidelines on radiation dose and dose-optimization strategies in cardiovascular CT. *J Cardiovasc Comput Tomogr*. 2011;5:198–224.
19. Min JK, Koo BK, Erglis A, Doh JH, Daniels DV, Jegere S, Kim HS, Dunning A, Defrance T, Leipsic J. Effect of image quality on diagnostic accuracy of noninvasive fractional flow reserve: results from the prospective multicenter international DISCOVER-FLOW study. *J Cardiovasc Comput Tomogr*. 2012;6:191–199.
20. Min JK, Taylor CA, Achenbach S, Koo BK, Leipsic J, Norgaard BL, Pijls NJ, De Bruyne B. Noninvasive fractional flow reserve derived from coronary CT angiography: clinical data and scientific principles. *JACC Cardiovasc Imaging*. 2015;8:1209–1222.
21. Mickey RM, Greenland S. The impact of confounder selection criteria on effect estimation. *Am J Epidemiol*. 1989;129:125–137.
22. Bursac Z, Gauss CH, Williams DK, Hosmer DW. Purposeful selection of variables in logistic regression. *Source Code Biol Med*. 2008;3:17.
23. DeLong ER, DeLong DM, Clarke-Pearson DL. Comparing the areas under two or more correlated receiver operating characteristic curves: a nonparametric approach. *Biometrics*. 1988;44:837–845.

24. Hetterich H, Jaber A, Gehring M, Curta A, Bamberg F, Filipovic N, Rieber J. Coronary computed tomography angiography based assessment of endothelial shear stress and its association with atherosclerotic plaque distribution in-vivo. *PLoS One*. 2015;10:e0115408.
25. Myers JG, Moore JA, Ojha M, Johnston KW, Ethier CR. Factors influencing blood flow patterns in the human right coronary artery. *Ann Biomed Eng*. 2001;29:109–120.
26. Death AK, Nakhla S, McGrath KC, Martell S, Yue DK, Jessup W, Celermajer DS. Nitroglycerin upregulates matrix metalloproteinase expression by human macrophages. *J Am Coll Cardiol*. 2002;39:1943–1950.
27. Galis ZS, Sukhova GK, Lark MW, Libby P. Increased expression of matrix metalloproteinases and matrix degrading activity in vulnerable regions of human atherosclerotic plaques. *J Clin Invest*. 1994;94:2493–2503.
28. Schoenhagen P, Vince DG, Ziada KM, Kapadia SR, Lauer MA, Crowe TD, Nissen SE, Tuzcu EM. Relation of matrix-metalloproteinase 3 found in coronary lesion samples retrieved by directional coronary atherectomy to intravascular ultrasound observations on coronary remodeling. *Am J Cardiol*. 2002;89:1354–1359.
29. Kolpakov V, Gordon D, Kulik TJ. Nitric oxide-generating compounds inhibit total protein and collagen synthesis in cultured vascular smooth muscle cells. *Circ Res*. 1995;76:305–309.
30. Casey PJ, Dattilo JB, Dai G, Albert JA, Tsukurov OI, Orkin RW, Gertler JP, Abbott WM. The effect of combined arterial hemodynamics on saphenous venous endothelial nitric oxide production. *J Vasc Surg*. 2001;33:1199–1205.
31. Ehara S, Kobayashi Y, Yoshiyama M, Shimada K, Shimada Y, Fukuda D, Nakamura Y, Yamashita H, Yamagishi H, Takeuchi K, Naruko T, Haze K, Becker AE, Yoshikawa J, Ueda M. Spotty calcification typifies the culprit plaque in patients with acute myocardial infarction: an intravascular ultrasound study. *Circulation*. 2004;110:3424–3429.
32. Motoyama S, Sarai M, Harigaya H, Anno H, Inoue K, Hara T, Naruse H, Ishii J, Hishida H, Wong ND, Virmani R, Kondo T, Ozaki Y, Narula J. Computed tomographic angiography characteristics of atherosclerotic plaques subsequently resulting in acute coronary syndrome. *J Am Coll Cardiol*. 2009;54:49–57.
33. Motoyama S, Ito H, Sarai M, Kondo T, Kawai H, Nagahara Y, Harigaya H, Kan S, Anno H, Takahashi H, Naruse H, Ishii J, Hecht H, Shaw LJ, Ozaki Y, Narula J. Plaque characterization by coronary computed tomography angiography and the likelihood of acute coronary events in mid-term follow-up. *J Am Coll Cardiol*. 2015;66:337–346.
34. Kenagy RD, Fischer JW, Davies MG, Berceli SA, Hawkins SM, Wight TN, Clowes AW. Increased plasmin and serine proteinase activity during flow-induced intimal atrophy in baboon PTFE grafts. *Arterioscler Thromb Vasc Biol*. 2002;22:400–404.
35. Choi BJ, Prasad A, Gulati R, Best PJ, Lennon RJ, Barsness GW, Lerman LO, Lerman A. Coronary endothelial dysfunction in patients with early coronary artery disease is associated with the increase in intravascular lipid core plaque. *Eur Heart J*. 2013;34:2047–2054.
36. Lavi S, Bae JH, Rihal CS, Prasad A, Barsness GW, Lennon RJ, Holmes DR Jr, Lerman A. Segmental coronary endothelial dysfunction in patients with minimal atherosclerosis is associated with necrotic core plaques. *Heart*. 2009;95:1525–1530.
37. Choi G, Lee JM, Kim HJ, Park JB, Sankaran S, Otake H, Doh JH, Nam CW, Shin ES, Taylor CA, Koo BK. Coronary artery axial plaque stress and its relationship with lesion geometry: application of computational fluid dynamics to coronary CT angiography. *JACC Cardiovasc Imaging*. 2015;8:1156–1166.